Capillary gravity waves: A "fixed-depth" analysis

F. Chevy and E. Raphaël

Laboratoire de Physique de la Matière Condensée
UMR CNRS 7125 and FR CNRS 2438
Collège de France, 75231 Paris Cedex 05, France

Abstract. – We study the onset of the wave resistance due to the generation of capillary gravity waves by a partially immersed moving object in the case where the object is held at a fixed immersion depth. We show that, in this case, the wave resistance varies continuously with the velocity, in qualitative accordance with recent experiments by Burghelea *et al.* (*Phys. Rev. Lett.*, **86** (2001) 2557).

Introduction. – The dispersive properties of capillary gravity waves are responsible for the complicated wave pattern generated at the free surface of a still liquid by a disturbance moving with a velocity V greater than the minimum phase speed $V_c = (4g\gamma/\rho)^{1/4}$, where g is the gravity, γ is the surface tension and ρ the density of the fluid [1]. The disturbance may be produced by a small object partially immersed in the liquid or by the application of an external surface pressure distribution [2]. The waves generated by the moving perturbation propagate momentum to infinity and, consequently, the disturbance experiences a drag $\boldsymbol{R}$ called the wave resistance [3]. For $V < V_c$, the wave resistance is equal to zero since, in this case, no propagating long-range waves are generated by the disturbance [4].

A few years ago, it was predicted that the wave resistance corresponding to a surface pressure distribution symmetrical about a point should be discontinuous at $V = V_c$ [5]. More precisely, if F_0 is the total vertical force exerted on the fluid surface, the wave resistance is expected to reach a finite value $R_c > 0$ for $V \to V_c^+$. For an object much smaller than the capillary length $\kappa^{-1} = \sqrt{\gamma/\rho g}$, the discontinuity R_c is given by

$$R_c = \frac{F_0^2}{2\sqrt{2}} \frac{\kappa}{\gamma}. \tag{1}$$

Experimentally, the onset of the wave resistance due to the generation of capillary gravity waves by a partially immersed moving object was studied recently by two independent groups [6, 7]. While Browaeys *et al.* [6] used a flexible wire and found a discontinuous behaviour of the wave resistance at $V = V_c$ [8], Burghelea *et al.* [7] used a bead immersed at a fixed depth and observed a smooth transition.

The discrepancy between the theoretical analysis of [5] and the experimental results of [7] might be due to the fact that the experimental setup of Burghelea *et al.* uses a feedback
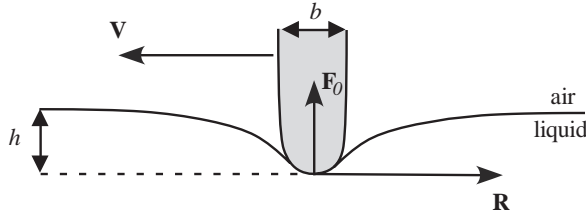
Fig. 1 – We study the behavior of a hydrophobic moving object of characteristic size b immersed at a depth h. The velocity of the object is V. We decompose the force exerted by the fluid on the object in a component orthogonal to the free surface (F_0) and a component parallel to it (R).

loop to keep the object at a constant depth while the analysis of [5] assumes that the vertical component F_0 of the force exerted by the disturbance on the fluid does not depend on the velocity V (we might call such an analysis a "fixed force" analysis). In order to check this proposition, we perform in this letter a "fixed-depth" calculation of the wave drag close to the onset threshold. A somewhat similar analysis was performed in the large velocity limit by Sun and Keller [9]. We will show that such a calculation indeed yields a cancellation of the vertical force at $V = V_c$, *i.e.* according to eq. (1), a smoothing of the discontinuity.

Model. –   We take the (x, y)-plane as the equilibrium surface of the fluid. The immersed object exerts a stress at the fluid surface that can be considered equivalent to a pressure field p [10] that travels over the surface with a velocity V in the x-direction (fig. 1). We assume $\hat{p}$ (the Fourier transform of p) to be of the form

$$\hat{p}(k_x, k_y) = F_0 \hat{\phi}(k), \tag{2}$$

where $k = \sqrt{k_x^2 + k_y^2}$ and $\hat{\phi}(0) = 1$. In this case, $\hat{p}$ is isotropic [11] and F_0 is the total vertical force exerted on the fluid.

Within the framework of Rayleigh's linearized theory of capillary gravity waves, the Fourier transform $\hat{\xi}(\boldsymbol{k})$ of the free surface displacement $\xi(\boldsymbol{r})$ is related to the pressure field through [12]

$$\hat{\xi}(k_x, k_y) = -F_0 \frac{k}{\rho} \left(\frac{\hat{\phi}(k)}{\omega_0^2(k) - 4\nu^2 k^3 q + (2\nu k^2 - i\boldsymbol{V} \cdot \boldsymbol{k})^2} \right), \tag{3}$$

where $\omega_0^2(k) = gk + \gamma k^3/\rho$ is the free dispersion relation, $q^2 = k^2 - i\boldsymbol{k} \cdot \boldsymbol{V}/\nu$ and $\nu = \eta/\rho$ is the kinematic viscosity of the fluid.

Let us suppose that the object is located at the origin of the moving frame. If h is its depth, the free surface displacement ξ must be $-h$ under the pinpoint (here we suppose the object sufficiently hydrophobic and h not to large so that the pinpoint does not pierce the surface). This leads to the following normalization condition:

$$\xi(\boldsymbol{0}) = \int \frac{\mathrm{d}^2 k}{(2\pi)^2} \, \hat{\xi}(\boldsymbol{k}) = -h. \tag{4}$$

The value of h as a function of F_0 can be readily calculated using eqs. (3) and (4):

$$h = \Xi(V) F_0, \tag{5}$$

with

$$\Xi(V) = \int \frac{\mathrm{d}^2 k}{(2\pi)^2} \frac{k}{\rho} \left(\frac{\hat{\phi}(k)}{\omega_0^2(k) - 4\nu^2 k^3 q^2 + (2\nu k^2 - i\boldsymbol{V} \cdot \boldsymbol{k})^2} \right). \tag{6}$$

Finally, the drag-force $\boldsymbol{R}$ is calculated by simply integrating the pressure force over the free surface [13],

$$\boldsymbol{R} = -\int \mathrm{d}^2 r \, p(\boldsymbol{r}) \boldsymbol{\nabla} \xi(\boldsymbol{r}) = -\int \frac{\mathrm{d}^2 k}{(2\pi)^2} \, i\boldsymbol{k} \hat{p}^*(\boldsymbol{k}) \hat{\xi}(\boldsymbol{k}). \tag{7}$$

This yields, using the explicit expression (3) for $\hat{\xi}$,

$$\boldsymbol{R} = F_0^2 \boldsymbol{\Lambda}(V), \tag{8}$$

with

$$\boldsymbol{\Lambda}(V) = \int \frac{\mathrm{d}^2 k}{(2\pi)^2 \rho} \left(\frac{i\boldsymbol{k}\boldsymbol{k}|\hat{\phi}(k)|^2}{\omega_0^2(k) - 4\nu^2 k^3 q^2 + (2\nu k^2 - i\boldsymbol{V} \cdot \boldsymbol{k})^2} \right). \tag{9}$$

According to eq. (8), the integral $\boldsymbol{\Lambda}$ describes the fixed-force behaviour of the wave resistance. Due to the symmetry of $\hat{\phi}$, $\boldsymbol{\Lambda}$ is parallel to $\boldsymbol{V}$ and we shall henceforth set $\boldsymbol{\Lambda} = \Lambda \boldsymbol{u}$, where $\boldsymbol{u} = \boldsymbol{V}/V$ is the unit vector parallel to the velocity of the object. The authors of [5] studied the properties of Λ in the case of a non-viscous fluid for which they showed that

a) $\Lambda = 0$ for $V < V_\mathrm{c}$;

b) Λ is discontinuous for $V \to V_\mathrm{c}^+$, with

$$\lim_{V \to V_\mathrm{c}^+} \Lambda = \Lambda_\mathrm{c} = \frac{1}{2\sqrt{2}} \frac{\kappa}{\gamma}; \tag{10}$$

c) in the large velocity limit

$$\Lambda \sim \frac{2\rho V^2}{3\pi\gamma^2}. \tag{11}$$

In the case of a fixed depth analysis, F_0 becomes a function of V. Using eqs. (5), we can rewrite the wave resistance as

$$\boldsymbol{R} = h^2 \frac{\boldsymbol{\Lambda}(V)}{\Xi^2(V)}. \tag{12}$$

In general, we have to rely on numerics to calculate the integrals Ξ and Λ. Typical results are presented in fig. 2 for an object of size 0.1 mm immersed in water, and for a step-like function $\hat{\phi}$ equal to 1 for $k < 1/b$ and 0 otherwise. We first observe in fig. 2(a) that Ξ increases sharply near the threshold. This leads to two rather different behaviours for Λ and R as shown in fig. 2(b): while Λ exhibits a discontinuity close to $V = V_\mathrm{c}$ [14], the fixed-depth wave drag $R = \Lambda/\Xi^2$ cancels smoothly at the critical velocity.

Inviscid flow. – The characteristic features displayed by the plots of fig. 2 can be captured by a zero-viscosity analysis. Setting $\nu = 0$, eq. (6) can be simplified as

$$\Xi = \mathcal{P} \int \frac{\mathrm{d}^2 k}{(2\pi)^2} \frac{k}{\rho} \left(\frac{\hat{\phi}(k)}{\omega_0^2(k) - (\boldsymbol{k} \cdot \boldsymbol{V})^2} \right), \tag{13}$$
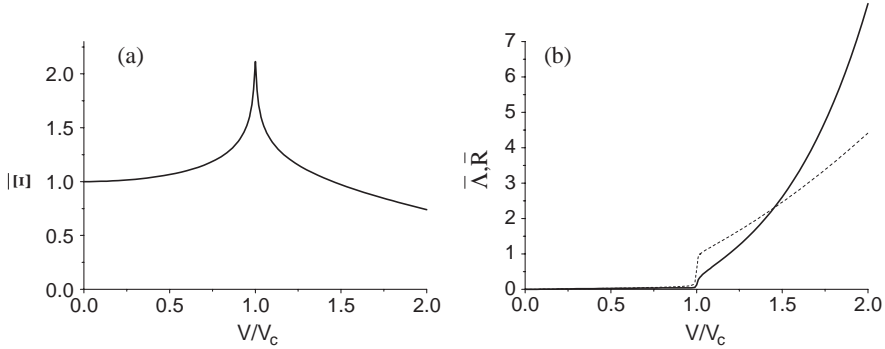
Fig. 2 – (a) Numerical calculation of the dimensionless integral $\bar{\Xi} = \Xi(V)/\Xi(0)$. (b) Comparison of $\bar{\Lambda}(V) = \Lambda(V)/\Lambda_c$ (dashed line) and $\bar{R} = \bar{\Lambda}/\bar{\Xi}^2$ (full line) describing, respectively, the fixed-force and fixed-depth behaviour of the wave resistance. We clearly see that contrary to the fixed-force analysis, the fixed-depth calculation does not yield any discontinuity at the threshold. Here $\nu = 10^{-6} \ \mathrm{m^2 \, s^{-1}}$, $\gamma = 72 \ \mathrm{mN \, m^{-1}}$, $\rho = 1000 \ \mathrm{kg \, m^{-3}}$ and $b = 0.1$ mm.

where $\mathcal{P}$ denotes the Cauchy principal value of the integral. The integral is calculated in polar coordinates (k, θ), where θ is the angle of $\boldsymbol{k}$ with respect to $\boldsymbol{V}$. Introducing the function G defined by

$$G(k) = \mathcal{P} \int_0^{2\pi} \frac{\mathrm{d}\theta}{2\pi} \left(\frac{1}{m_k^2 - 2\mathcal{M}^2 \cos^2(\theta)} \right), \tag{14}$$

where $m_k^2 = k/\kappa + \kappa/k$ and $\mathcal{M} = V/V_c$ is the "Mach" number, eq. (13) can then be rewritten as

$$\Xi = \frac{1}{\gamma\kappa} \int_0^\infty \frac{\mathrm{d}k}{2\pi} \hat{\phi}(k) G(k). \tag{15}$$

Using the residue theorem [15], we get

$$G(k) = \frac{1}{\sqrt{m_k^2(m_k^2 - 2\mathcal{M}^2)}} \Theta(m_k^2 - 2\mathcal{M}^2), \tag{16}$$

where Θ is the Heaviside step function. The variations of m_k^2 with k are plotted in fig. 3: m_k^2 reaches its minimum value $(m_k^2)_{\min} = 2$ for $k = \kappa$. It shows that the equation $2\mathcal{M}^2 - m_k^2 = 0$ has two solutions, k_1 and k_2, with $k_1 < \kappa < k_2$, if V is larger than the critical velocity V_c, and none if $V < V_c$.

For $V > V_c$, Ξ evaluates to

$$\Xi = \frac{1}{\gamma\kappa} \left[\int_0^{k_1} \frac{\mathrm{d}k}{2\pi} \frac{\hat{\phi}(k)}{\sqrt{m_k^2(m_k^2 - 2\mathcal{M}^2)}} + \int_{k_2}^\infty \frac{\mathrm{d}k}{2\pi} \frac{\hat{\phi}(k)}{\sqrt{m_k^2(m_k^2 - 2\mathcal{M}^2)}} \right]. \tag{17}$$

The above integrals can be calculated in the two limiting cases $\mathcal{M} \approx 1$ (*i.e.* $V \approx V_c$) and $\mathcal{M} \gg 1$ (*i.e.* $V \gg V_c$).

For large $\mathcal{M}$, the integrals are restricted to either large or small values of k. If $\hat{\phi}$ vanishes faster than $1/k$ for large k, we can show that the small-k contribution dominates. In this region, the dispersion relation is dominated by gravity waves, so that we can approximate m_k^2 by k/κ. A straightforward calculation then yields the following asymptotic expansion for Ξ:

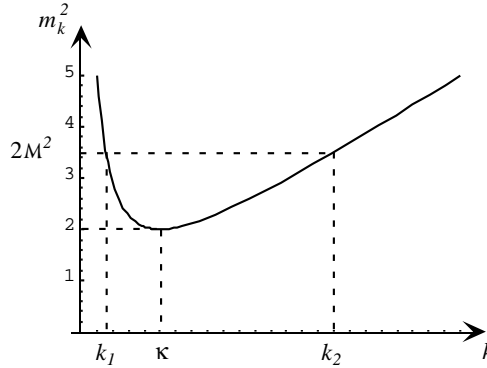$$\Xi \sim \frac{1}{6\pi\gamma} \left(\frac{V_c}{V} \right)^4. \tag{18}$$

Fig. 3 – Variations of m_k^2 (see text) with k. Since m_k^2 reaches a minimum for $k = \kappa$ with $m_\kappa^2 = 2$, the equation $m_k^2 = 2\mathcal{M}^2$ presents solutions for $\mathcal{M} > 1$. In this case, there are two possible values, k_1 and k_2 with $k_1 < \kappa < k_2$.

Combining this result with (11) and 12, we get

$$R \sim 12\pi\rho h^2 \frac{V^{10}}{V_c^8}.$$

Let us now focus on the case V close to V_c. We set

$$\widetilde{\Xi}_1 = \int_0^{k_1} \frac{\mathrm{d}k}{2\pi} \frac{\hat{\phi}(k)}{\sqrt{m_k^2(m_k^2 - 2\mathcal{M}^2)}},$$

and

$$\widetilde{\Xi}_2 = \int_{k_2}^\infty \frac{\mathrm{d}k}{2\pi} \frac{\hat{\phi}(k)}{\sqrt{m_k^2(m_k^2 - 2\mathcal{M}^2)}}.$$

Using the fact that k_1 and k_2 are the roots of $m_k^2 = 2\mathcal{M}^2$, we can rewrite $\widetilde{\Xi}_1$ as

$$\widetilde{\Xi}_1 = \int_0^{k_1} \frac{\mathrm{d}k}{2\pi} \frac{k\hat{\phi}(k)}{\sqrt{(k^2/\kappa^2)(k - k_1)(k - k_2)}}.$$

When $V \to V_c$, the $(k - k_1)(k - k_2)$ term cancels in $k = \kappa$. Since all other terms are regular, we can write at the leading order

$$\widetilde{\Xi}_1 \sim \kappa \frac{\hat{\phi}(\kappa)}{\sqrt{2}} \int_0^{k_1} \frac{\mathrm{d}k}{2\pi} \frac{1}{\sqrt{(k - k_1)(k - k_2)}}.$$

This latter integral is readily calculated and gets a very simple form in the limit $V \to V_c$:

$$\widetilde{\Xi}_1 \sim \kappa \frac{\hat{\phi}(\kappa)}{\sqrt{2}} \ln(k_2 - k_1) \sim \kappa \frac{\hat{\phi}(\kappa)}{2\sqrt{2}} \ln(\mathcal{M} - 1).$$

Since m_k^2 is invariant by the transformation $k/\kappa \to \kappa/k$, Ξ_1 and Ξ_2 have the same asymptotic behaviour for $V \to V_c$. In this limit $\Xi = \left(\widetilde{\Xi}_1 + \widetilde{\Xi}_2\right)/\gamma\kappa \approx 2\widetilde{\Xi}_1/\gamma\kappa$, hence

$$\Xi \sim \frac{1}{2\pi\sqrt{2}\gamma} \hat{\phi}(\kappa) \ln(\mathcal{M} - 1). \tag{19}$$

For an object of size b, the width of $\hat{\phi}$ is about $1/b$. If we choose $b \ll \kappa^{-1}$, we can approximate $\hat{\phi}(\kappa)$ by $\hat{\phi}(0) = 1$. Equation (19) then takes the following form [16]:

$$\Xi \sim \frac{1}{2\pi\sqrt{2}\gamma} \ln(\mathcal{M} - 1) \sim \frac{1}{2\pi\sqrt{2}\gamma} \ln\left(\frac{V - V_c}{V_c}\right). \tag{20}$$

Combining eqs. (10) and (20), we see that slightly above the threshold, the wave resistance behaves like

$$R \sim \frac{4\pi^2}{\sqrt{2}} \left(\frac{\gamma\kappa h^2}{\ln^2(V/V_c - 1)}\right). \tag{21}$$

Equation (21) constitutes the main result of this paper. First, we notice that for small objects this relation is independent of the shape of the pressure field. Second, and more important, it shows that the wave resistance R cancels out at $V = V_c$. This smearing is due to the cancellation of the vertical force F_0 near the threshold that we get from the behaviour of Ξ.

Comparison with experiments. – Comparison of eq. (21) and the result of [5] proves that the behaviour of the wave resistance is strongly dependent on the conditions in which the experiments are performed and suggests that a full test of Raphaël and de Gennes' model requires a measurement of both R and F_0.

The model proposed here roughly reproduces the conditions of Burghelea's setup. It leads indeed to a smooth cancellation of the drag at the threshold but accordance remains only qualitative. Indeed, authors of [17] find the following scaling for the wave drag:

$$R_{\exp} \sim F_c \rho (gh)^{3/2} \frac{b^2}{\nu\gamma} f(V/V_c),$$

where F_c is the Stockes drag at threshold and h the width of the channel. Assuming the simple law $F_c \sim \rho\nu b V_c$, we get

$$R_{\exp} \sim \left(\frac{\rho^7 g^7}{\gamma^3}\right)^{1/4} h^{3/2} b^3 f(V/V_c), \tag{22}$$

which differs from the scaling of eq. (21). It should be emphasized that (22) involves finite-size effects (due to the presence of the width h of the channel) and is hence beyond the scope of our model which assumes an infinite geometry.

In this respect comparison with [6] is more involved and would require further theoretical studies to be fully understood. Indeed, due to the setup design (an immersed wire, wetted by the liquid and the deflection of which measures the wave resistance), it cannot be described by any of the two simple types of models presented here (constant depth or constant force).

Conclusion. – In this paper we have shown that in a fixed-depth situation the discontinuity of the drag force calculated in [5] vanishes and is replaced by a smooth variation, in accordance with the experimental results found in [7]. A quantitative comparison between the present analysis and the data of ref. [7] is however more involved, since experiments from [7] were performed in narrow channel geometry [17] and would require the description of the reflections of the waves on the walls of the channel. Further study would also be required to understand the role of wetting of the liquid on the object in the variation of the wave drag. The present calculation suggests nevertheless that to fully test relation (1), experiments need to be devised that would measure both R and F_0.

$* * *$

We wish to thank J. Browaeys, P.-G. de Gennes and D. Richard for very helpful discussions, as well as V. Steinberg for sending us his experimental data prior to publication.

REFERENCES

[1]   Lighthill J., in *Waves in Fluids* (Cambridge University Press) 1978.
[2]   Lord Kelvin, *Proc. R. Soc. London, Ser. A*, **42** (1887) 80.
[3]   See, *e.g.*, Debnath L., in *Nonlinear Water Waves* (Academic Press Inc., San Diego) 1994.
[4]   Note that for a viscous fluid, the moving perturbation is also subjected to the usual Stokes drag, for both $V < V_c$ and $V > V_c$.
[5]   Raphaël E. and de Gennes P. G., *Phys. Rev. E*, **53** (1996) 3448.
[6]   Browaeys J., Bacri J.-C., Perzynski R. and Shliomis M., *Europhys. Lett.*, **53** (2001) 209.
[7]   Burghelea T. and Steinberg V., *Phys. Rev. Lett.*, **86** (2001) 2557.
[8]   We shall see later that the comparison of the data from [6] and the theoretical prediction requires some care, and the experimental observation of a discontinuous behaviour of the wave-resistance is not a proof of the validity of eq. (1).
[9]   Sun Shu-Ming and Keller J., *Phys. Fluids*, **13** (2001) 2146.
[10] Not that this assumption is not entirely correct in the presence of viscosity since it leads to a slip of the object with respect to the fluid surface. In this case, a force field parallel to the free surface should also be added. However, this new term leads to the usual Stokes drag, that is subtracted from experimental results, and so can be omitted in our analysis.
[11] This latter hypothesis is not too restrictive in the case of very small object.
[12] This generalizes the 2D result of Richard D. and Raphaël E., *Europhys. Lett.*, **48** (1999) 53.
[13] Havelock T. H., *Proc. R. Soc. London, Ser. A*, **95** (1918) 354.
[14] For an inviscid fluid, this increase is actually a discontinuity. For high viscosities, we have observed no noticeable accident of $\mathbf{\Lambda}$ for V close to V_c.
[15] See, *e.g.*, Riley K. F., Hobson M. P. and Bence S. J., in *Mathematical Methods for Physics and Engineering* (Cambridge University Press) 1998.
[16] A more precise evaluation of the validity range would require to know the actual shape of $\hat{\phi}$ and its evolution with the object velocity.
[17] Burghelea T. and Steinberg V., *Phys. Rev. E*, **66** (2002) 051204.